NACA

RESEARCH MEMORANDUM

INTERFEROMETRIC OBSERVATION OF FLOW ABOUT AN ISENTROPIC (REVERSE PRANDTL-MEYER STREAMLINE) COMPRESSION WEDGE AT MACH 3.0

By James F. Connors, Richard R. Woollett, and Robert E. Blue

Lewis Flight Propulsion Laboratory
Cleveland, Ohio

NATIONAL ADVISORY COMMITTEE FOR AERONAUTICS

WASHINGTON

March 28, 1955
Declassified February 8, 1957

NATIONAL ADVISORY COMMITTEE FOR AERONAUTICS

RESEARCH MEMORANDUM

INTERFEROMETRIC OBSERVATION OF FLOW ABOUT AN ISENTROPIC (REVERSE PRANDTL-MEYER STREAMLINE) COMPRESSION WEDGE AT MACH 3.0

By James F. Connors, Richard R. Woollett, and Robert E. Blue

SUMMARY

An interferometric study was made of the flow over a two-dimensional isentropic (reverse Prandtl-Meyer streamline) compression surface at a Mach number of 3.0. The flow field was essentially that of a strong-branch-shock configuration resulting from a surface flow turning that corresponded to an empirical limiting value of free-stream normal-shock pressure rise.

Based on a mapping of constant-density contour lines, a comparison was made between the experimental results and those predicted from theoretical flow considerations. The boundary layer that developed along the wedge surface caused the flow to deviate from the theoretical streamline contour and thus prevented the compression waves from focussing at a common intersection point. Concomitantly, the predicted modifications of the flow due to the theoretical boundary-layer displacement thickness agreed well with experiment. The locations of the strong shock and the sonic point along the vortex sheet, as determined from an experimental Mach number distribution, showed fair agreement with theoretical estimates for detached waves ahead of blunt two-dimensional bodies.

INTRODUCTION

When a supersonic stream is decelerated by means of a focussed isentropic-compression surface to a pressure larger than can be matched by an oblique shock, a strong branch-shock configuration originates near the intersection point, as shown in reference 1. It was noted that, for all external compression inlets above a Mach number of 2.2, a practical design limitation exists on the degree of compressive turning that can be efficiently imposed upon the flow. This proposed limit corresponds to the condition producing a static-pressure rise across the supersonic isentropic-compression field equal to that across a free-stream normal shock. For configurations designed for and in

excess of this limit, there appears to be no adequate theoretical description of the resultant strong-shock structures and mixed-flow fields.

Therefore, in an effort to acquire further understanding of the flow mechanisms involved, a study was initiated of the flow fields about a compression surface with turning corresponding to the proposed limit. At a Mach number of 3.0, a two-dimensional isentropic (reverse Prandtl-Meyer streamline) compression surface was used. Observation of the resulting flow was made with the aid of a Mach-Zehnder interferometer. This report presents an analysis of the data thus obtained.

APPARATUS AND PROCEDURE

The investigation was conducted in the Lewis 4- by 10-inch wind tunnel at a Mach number of 3.0. The air was dried to a dew-point temperature of approximately -20° F and was maintained at a total pressure of 16.3 pounds per square inch absolute and a total temperature of 100° F upstream of the tunnel nozzle. In the test chamber the Reynolds number was approximately 2.4×10^6 per foot.

The model which completely spanned the tunnel consisted simply of a contoured (reverse Prandtl-Meyer streamline) compression wedge with an initial angle of approximately 6°. With isentropic compression, the main flow could be reduced on the basis of theoretical flow turning from a free-stream Mach number of 3.0 down to a final Mach number of approximately 1.5 and a local-to-free-stream density ratio ρ/ρ_0 of 5.6. This turning corresponds to the proposed normal-shock pressure limit.

The interference pictures were obtained with a conventional Mach-Zehnder interferometer with the use of the mercury green line 5461 Å from a microsecond flash of a high-pressure mercury arc. The fringes were focused on the midspan plane of the model in order to minimize refraction errors (ref. 2). An infinite fringe adjustment would have been the simplest to analyze since each fringe in the flow picture would then be an isopycnic line if refraction corrections were negligible. However, because the tunnel windows of rolled optical plate glass were slightly inferior in quality, an infinite fringe could not be obtained. A wide approximately vertical fringe adjustment (fig. 1) was used so that corrections for variations in the no-flow fringe straightness could be applied in evaluating the flow picture. Except for this one variation, the evaluation procedure was conventional and may be found in any of a number of references (e.g., ref. 3).

An error due to temperature gradients in the glass windows can result from increased heat transfer at the junction of the full-span

steel model and the tunnel windows. The tunnel was therefore operated at a condition wherein the recovery temperature would be close to the room temperature. As a result, all surface temperature gradients were minimized; the associated error was assumed to be negligible.

No attempt was made to correct the density contours for light-refraction errors. The density gradients were not large enough to cause an appreciable error except in the regions immediately surrounding the main shock intersection and near the model surface at the shoulder where the flow reexpands.

RESULTS AND DISCUSSION

The resulting interferogram for flow about a contoured compression wedge at a Mach number of 3.0 is presented in figure 2. As in the usual isentropic inlet application, the wedge was initially designed so that the compression waves would coalesce at a common focal point. The resulting flow configuration was essentially that of a branch-shock structure, the upper leg of which was initially of the strong-shock family.

In the evaluation of this interferogram, the boundary layer on the tunnel windows caused the greatest uncertainty. The pressure rise over the contoured portion of the wedge undoubtedly separated and caused a rapid rate of growth of the side-wall boundary layer either ahead of or along the model. The exact magnitude of the error could be obtained only by probing the side-wall boundary layer and applying the correction discussed in reference 4. Since no such measurements were made, it must be kept in mind that the density evaluation will include an axial decrease in density which did not exist in the actual flow. For a 50-percent thickening of the side-wall boundary layer, the error would be approximately 3 percent.

The apparent thickness of the strong shock can also be attributed to the effect of the pressure rise feeding upstream through the side-wall boundary layer. This thickening is manifested as a density change in the stream ahead of the shock, thereby giving the shock the observed thickness.

Subject to these limitations, a density map of the flow field was computed and is presented in figure 3. The data points and solid lines represent experimental values of constant-density ratios (local-to-free-stream static density) that were derived from the interferogram evaluation. The maximum amount of compression indicated by the experimental data ($\rho/\rho_0 = 4.9$) was less than the design value ($\rho/\rho_0 = 5.6$). In figure 4 the theoretical, inviscid, reverse Prandtl-Meyer flow values are presented and it is shown that the experimental main shock intersection is located somewhat above the theoretical focal point.

As shown on figure 3, an appreciable boundary layer developed along the wedge surface. The boundary layer depicted on the density map corresponded to the observed inflection points of the interference fringes (fig. 2). At a station along the contoured surface (where $\rho/\rho_0 \sim 3.0$) the magnitude of the total boundary-layer thickness checked roughly with that predicted for turbulent flow (ref. 5), assuming a seventh-power profile to be maintained over the entire distance from the leading edge. The transition from laminar to turbulent flow was not defined. As the boundary layer approached the expansion region on the shoulder, there appeared to be a pronounced thinning, probably due to the influence of the favorable pressure gradient. This thinning may cause the final effective compressive-turning angle to be somewhat less than the designed geometric maximum surface angle and may thereby account, in part, for the low value of compression realized experimentally. Hence, the qualitative over-all effect of the boundary layer was to produce a more rapid compression on the initial part of the wedge than the inviscid design theory prescribed and less compression on the rearward portion.

Again by assuming the boundary layer to be turbulent and to have a seventh-power profile, a displacement thickness was calculated (ref. 5) in order to approximate the effective flow surface. From this displacement surface, characteristics were calculated in order to indicate, at least qualitatively, the resulting theoretical pattern of the flow field (fig. 4). The agreement with the experimental results was very good. As shown in figure 4 and particularly in figure 5, the displacement effect of the boundary layer was to unfocus the characteristics with a general dispersion very much like the pattern of experimental isopycnic lines. On the forward portion of the wedge, the displacement-surface characteristics tended to steepen and coalesce and thus appeared to account in part for the location of the experimental main shock intersection above the theoretical focal point for inviscid flow.

Above this main shock intersection is located the strong shock, which forms the upper leg of the branch configuration. The remaining downstream components (the shock reflection and the vortex sheet) are also rather well defined by the local density changes (fig. 3) occurring across them. The slight increase in density that the flow encountered through the shock reflection identifies it as a weak compression wave. Across the vortex sheet, the density change is somewhat more pronounced with the lower densities occurring on the side facing the strong shock. The general shape of this vortex sheet is also of interest. In the immediate vicinity of the shock the vortex line is somewhat S-shaped because the subsonic flow field behind the strong shock is reaccelerated back to supersonic speeds. This was much like the patterns observed in reference 1 for the overcompressed configurations. Again, the maximum slope of the vortex sheet exceeded the detachment angle corresponding to the free-stream Mach number ($\lambda = 34^\circ$) by as much as 5°. As this

shear layer progressed downstream, it became increasingly thicker as a result of the mixing process taking place between the two adjacent streams.

Mach number distributions based on some simplifying assumptions are presented in figure 4. The Mach number variation along the upper boundary of the vortex sheet was calculated from the experimental density ratios of figure 3 with the assumption of free-stream normal-shock total-pressure recovery and constant total pressure along a streamline corresponding to the outer edge of the vortex sheet. The location of the sonic point thus obtained checked very closely with that given by a line at the free-stream detachment angle drawn tangent to the vortex sheet. The methods of reference 6 were further employed to determine the approximate form and location of a detached shock wave corresponding to flow ahead of a blunt two-dimensional body having the shape of the experimental vortex sheet. Agreement with the experimental strong shock was fair. Thus, the location and form of the strong wave appeared to be determined primarily by the shape of the vortex sheet which, in turn, would be determined by the expansion characteristics originating at the shoulder of the model.

Mach number distributions along the lower edge of the vortex sheet were derived with two different assumptions. The first was that the static pressure was constant across the shear layer. This information together with the experimental density ratios yielded the indicated first set of values of Mach number given for each point. Corresponding to this distribution, there was a decreasing total-pressure differential across the vortex sheet with distance downstream of the intersection. The indicated second set of values of Mach number at these points was computed from the local densities with the total-pressure assumed constant along the lower edge of the vortex sheet. This value was that previously calculated at the station nearest the shock intersection ($M = 1.50$) by assuming the static pressure constant across the shear layer. In each case, the flow was accelerated along both sides of the vortex sheet as a result of the flow expansion around the wedge shoulder. As shown by the Mach number distributions along the lower edge of the vortex line, the assumption of constant total pressure indicated a faster acceleration of the flow than the assumption of constant static pressure across the discontinuity. Because of the thickness of this mixing zone downstream of the shock intersection, it was not clear that either of these conditions holds; but, in general, the assumption of equal static pressures on the two sides of the vortex seems more plausible.

Across the shock reflection, Mach numbers were estimated from the experimental density ratios by assuming no upstream total-pressure loss other than the initial leading-edge shock loss. Corresponding flow-deflection angles through the shock reflection were on the order of

3° to 4° with a trend to decrease in value as the upstream Mach number was increased by the shoulder expansion waves.

CONCLUDING REMARKS

At Mach number 3.0 an interferometric analysis was made of the flow about an isentropic (reverse Prandtl-Meyer streamline) compression wedge with a surface flow-turning angle corresponding to a limiting value of free-stream normal-shock pressure rise. For the resulting strong-branch-shock configuration, a map of constant-density contour lines was made and compared with that predicted from theoretical flow considerations. Because of the displacement effect of the surface boundary layer, the flow deviated slightly from the theoretical streamline contour and caused a general dispersion or unfocussing of the compression characteristics. The predicted modifications of the flow due to the theoretical boundary-layer displacement thickness agreed well with experiment.

By assuming the vortex sheet analagous to a blunt two-dimensional body, some correlation between experiment and theoretical estimates for detached waves was obtained with regard to the locations of the strong shock and a sonic point along the vortex sheet as determined from experimental Mach number distributions. This correlation showed that the form and location of the strong bow wave was determined primarily by the shape of the vortex sheet originating downstream of the shock intersection.

Lewis Flight Propulsion Laboratory
National Advisory Committee for Aeronautics
Cleveland, Ohio, January 27, 1955

REFERENCES

1. Connors, James F., and Woollett, Richard R.: Characteristics of Flow About Axially Symmetric Isentropic Spikes for Nose Inlets at Mach Number 3.85. NACA RM E54F08, 1954.

2. Howes, Walton L., and Buchele, Donald R.: A Theory and Method for Applying Interferometry to the Measurement of Certain Two-Dimensional Gaseous Density Fields. NACA TN 2693, 1952.

3. Ladenburg, R., and Bershader, D.: Optical Studies of Boundary Layer Phenomena on a Flat Plate at Mach Number 2.35. Palmer Phys. Lab., Princeton Univ., Dec. 15, 1952. (Contract N6ori-105, Task II.)

4. Blue, Robert E.: Interferometer Corrections and Measurements of Laminar Boundary Layers in Supersonic Stream. NACA TN 2110, 1950.

5. Tucker, Maurice: Approximate Calculation of Turbulent Boundary-Layer Development in Compressible Flow. NACA TN 2337, 1951.

6. Moeckel, W. E.: Approximate Method for Predicting Form and Location of Detached Shock Waves Ahead of Plane or Axially Symmetric Bodies. NACA TN 1921, 1949.

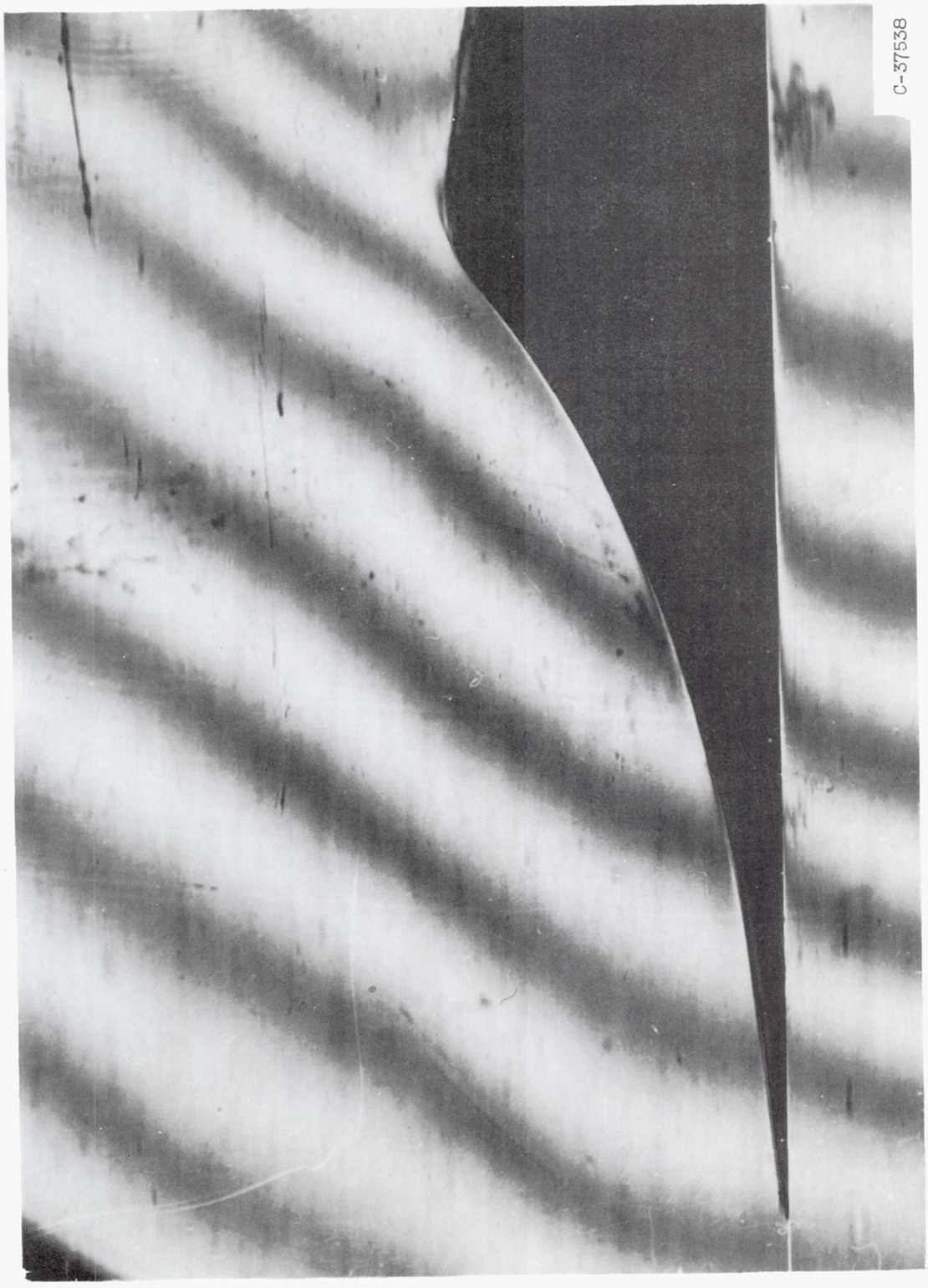

Figure 1. - No-flow interferogram.

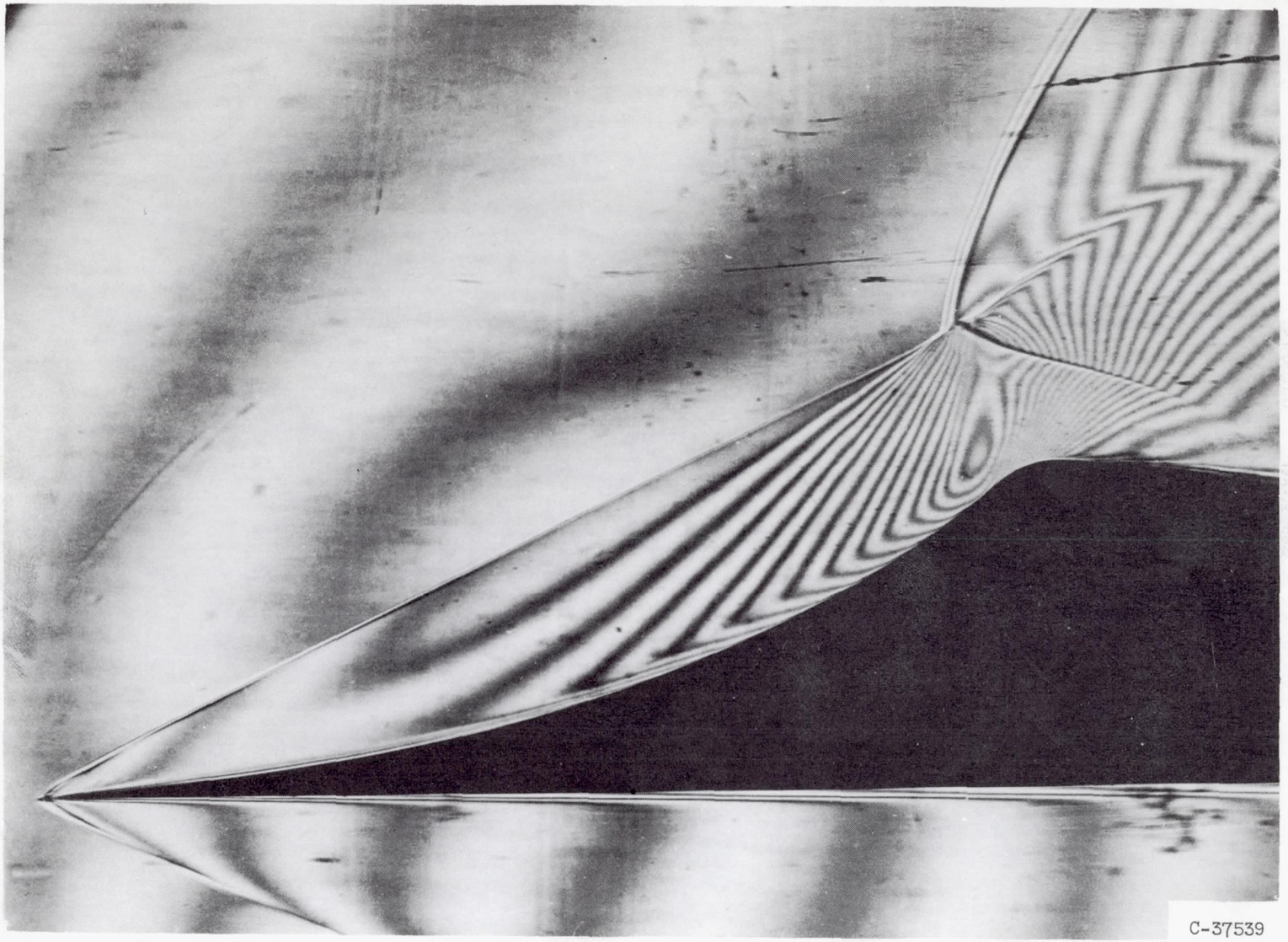

Figure 2. - Flow interferogram. Free-stream Mach number, 3.0.

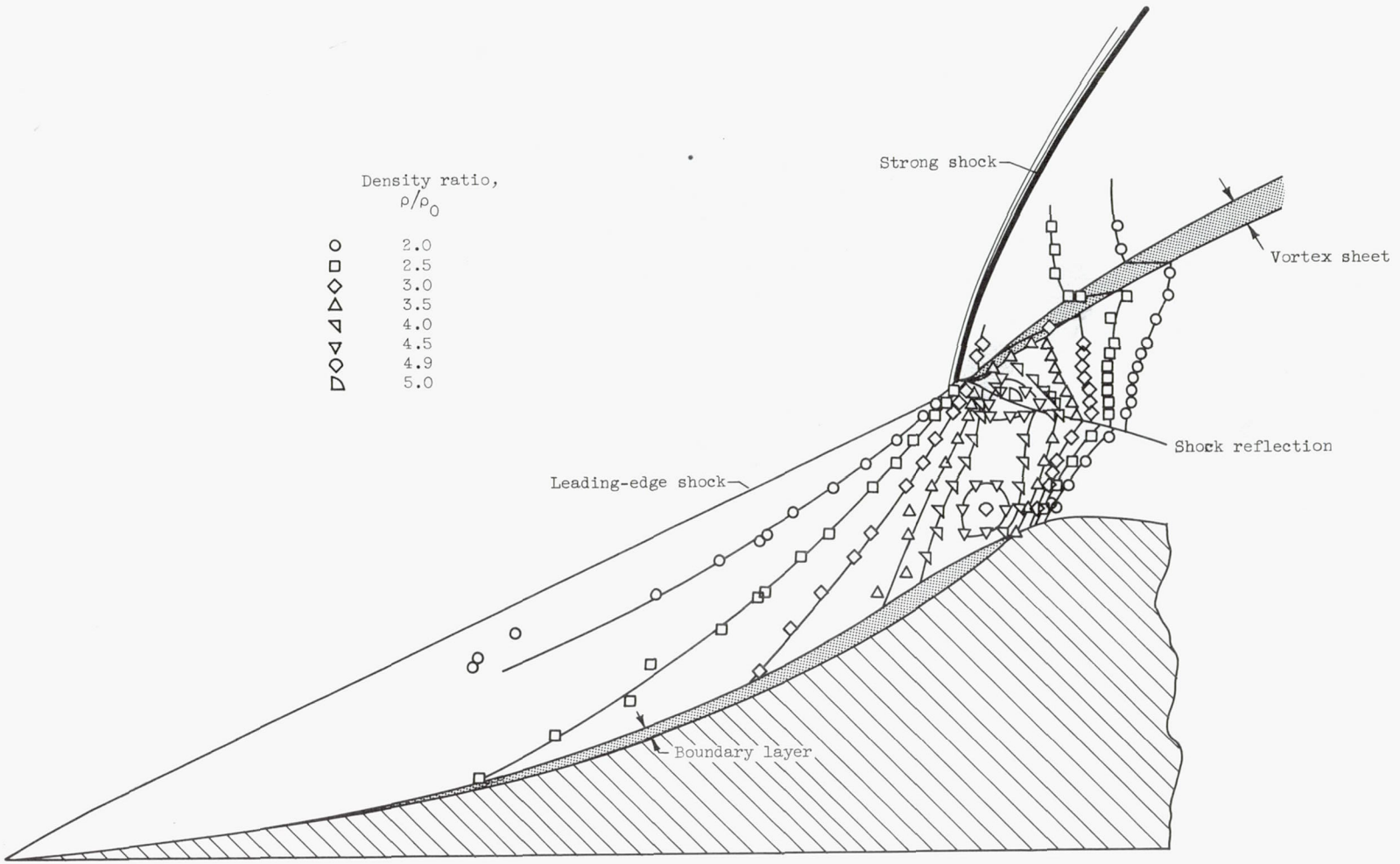

Figure 3. - Experimental density contour map of flow field about isentropic compression wedge at Mach number of 3.0.

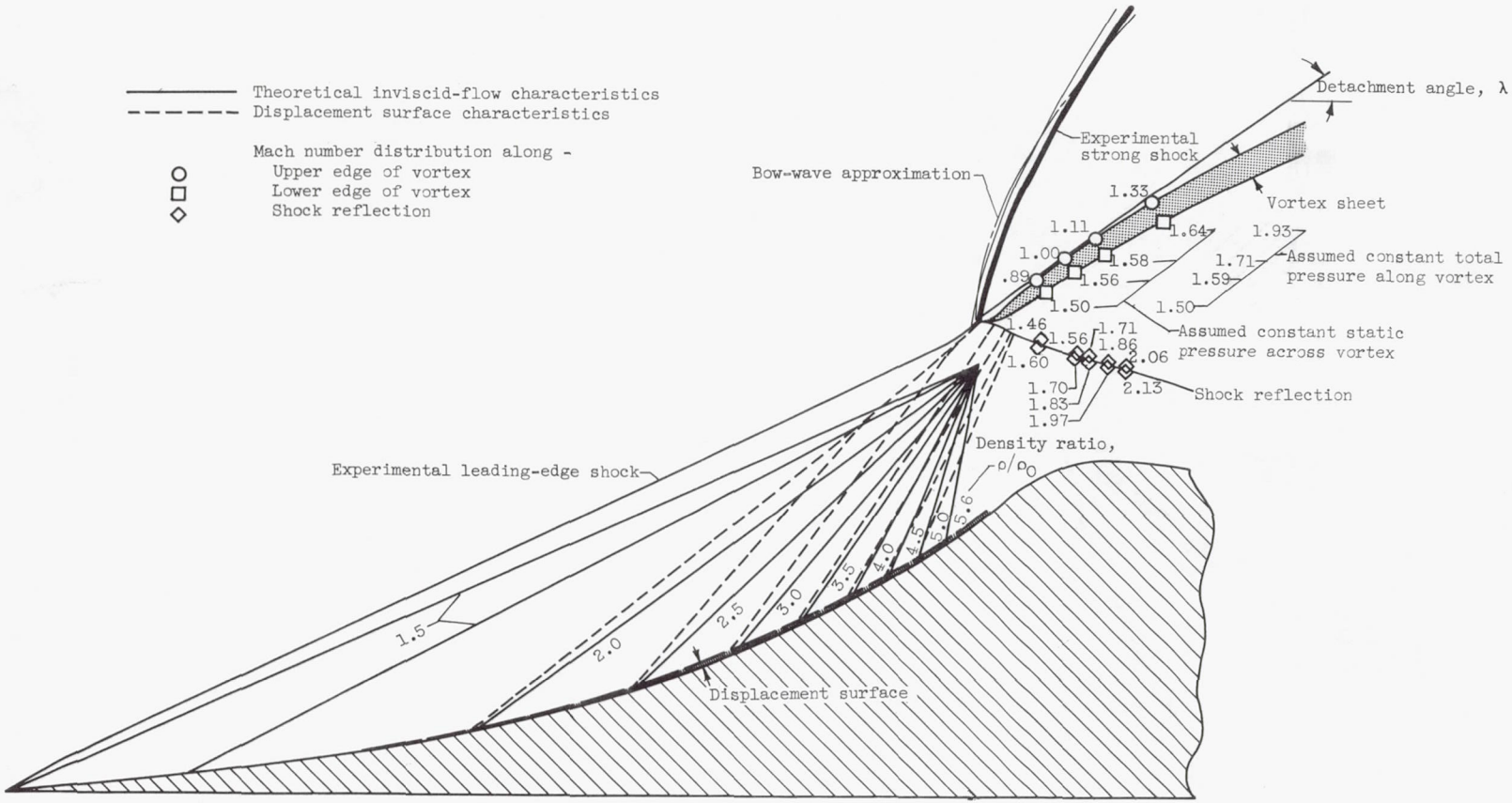

Figure 4. - Analysis of experimental flow field and correlation with theoretical approximations.

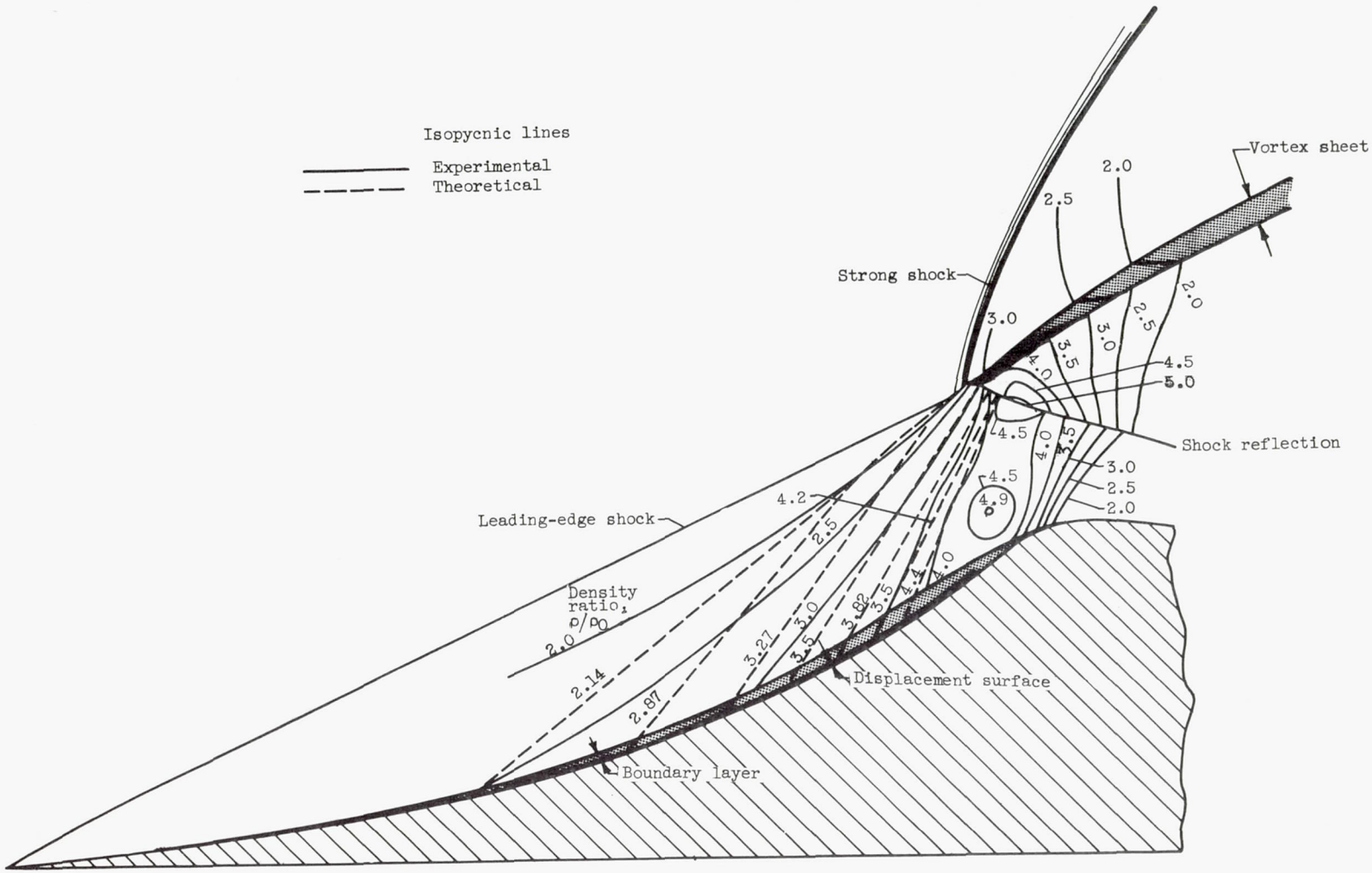

Figure 5. - Comparison of experimental and theoretical isopycnic lines.

NACA - Langley Field, Va